DIRECT NUMERICAL SIMULATION OF MIXING IN A PLANE COMPRESSIBLE AND TURBULENT WALL JET

Daniel Ahlman, Geert Brethouwer, Arne V. Johansson
Department of Mechanics,
Royal Institute of Technology
SE-100 44 Stockholm, Sweden
ahlman@mech.kth.se

ABSTRACT

Direct numerical simulation (DNS) is used to simulate the mixing of a passive scalar in a plane compressible and turbulent wall jet. The Mach number of the jet is $M = 0.5$ at the inlet. The downstream development of the jet is studied and compared to experimental data. Mixing in the inner and outer shear layers of the wall jet is investigated through scalar fluxes, the probability density function of the scalar concentration and the joint probability density function of the wall normal velocity fluctuation and the scalar concentration.

INTRODUCTION

A plane wall jet is obtained by supplying momentum to a fluid along a wall in such a way that the velocity of the fluid over some distance from the wall supersedes that of the ambient flow. This flow configuration has historically been used extensively both in engineering applications and in fundamental research. The basic structure of a turbulent wall jet can be described as composed of two shear layers of different character. The inner part, reaching from the wall to the point of maximum streamwise velocity, resembles a thin boundary layer, while the outer part, reaching from the outer position of the inner layer to the ambient fluid, can be characterized as a free shear flow. A consequence of the double shear layer structure is that properties such as mixing and momentum transfer exhibit distinctively different character in the two shear layers.

For engineering purposes wall jets are used in a wide range of applications. Many of these applications apply wall jets to modify heat and mass transfer close to walls. Well known examples of these are i.e. in film-cooling of leading edges of turbine blades and in automobile demisters. In the first applications, the purpose is to use a cool layer of fluid to protect the solid surface from the hot external stream, while in the case of the demister, warm jet fluid is used to heat the inside of the wind shield to keep it free from condensation. The characteristic feature controlling the transfer processes in the mentioned applications is turbulent mixing in the vicinity of walls. However the mixing processes in this region are presently not fully understood and it is therefore of interest to add to this knowledge. An extended understanding of the mixing properties close to walls is also of relevance for applications containing combustion. In most combustion systems, such as in internal combustion engines and in gas turbines, part of the combustion will inevitably take place in the vicinity of and be influenced by walls. To be able to understand and accurately model combustion in this region, it is highly relevant to study the present mixing processes and how they are influenced by the presence of the wall.

Owing to the numerous applications of wall jets, the literature concerning experimental investigations is vast. The published material up to 1980 have meritoriously been compiled and critically reviewed by Launder and Rodi (1981,1983). Recent experimental studies include the work by Wygnanski et al. (1992), and Eriksson et al. (1998). Concerning the self-similarity of the wall jet, George et al. (2000) have proposed a new theory for the scaling of the inner and outer layers of the wall jet. The evolution and mixing of scalars in a plane jet, with no wall present, have been studied by means of DNS by Stanley et al. (2002). They studied the mixing of a passive scalar and found their simulation to compare well with classical experimental data. Concluding the brief background on previous research efforts, it can be said that little is still known of the mixing processes present in the plane wall jet.

In the present study, we analyze the mixing processes in a two-dimensional, compressible and turbulent wall jet, by means of three-dimensional DNS. The research is part of an ongoing project with the aim of developing a simulation code for DNS of reactive flows with an emphasis on wall effects.

GOVERNING EQUATIONS

Since realistic simulations of reactive flows involve heat release and considerable density fluctuations, the fully compressible formulation of the fluid dynamics problem is used. The equations employed for conservation of mass, momentum and energy (see Poinsot and Veynante) are

$$\frac{\partial \rho}{\partial t} + \frac{\partial \rho u_j}{\partial x_j} = 0, \tag{1}$$

$$\frac{\partial \rho u_i}{\partial t} + \frac{\partial \rho u_i u_j}{\partial x_j} = -\frac{\partial p}{\partial x_i} + \frac{\partial \tau_{ij}}{\partial x_j}, \tag{2}$$

$$\frac{\partial \rho E}{\partial t} + \frac{\partial \rho E u_j}{\partial x_j} = -\frac{\partial q_j}{\partial x_j} + \frac{\partial (u_i(\tau_{ij} - p\delta_{ij})}{\partial x_j}, \tag{3}$$

where ρ is the mass density of the fluid, u_i denotes the velocity components, p is the pressure and $E = (e + 1/2 u_i u_i)$ is the total energy. The fluid is considered to be Newtonian with a zero bulk viscosity, for which the general form of the viscous stress holds as

$$\tau_{ij} = -\frac{2}{3}\mu \frac{\partial u_k}{\partial x_k}\delta_{ij} + \mu\left(\frac{\partial u_i}{\partial x_j} + \frac{\partial u_j}{\partial x_i}\right), \tag{4}$$

where μ is the dynamic viscosity. The heat diffusion is approximated using Fourier's law for the heat fluxes $q_i = -\lambda \partial T/\partial x_i$ where λ is the coefficient of thermal conductivity and T is the

temperature. In the simulation a Prandtl number of one,

$$Pr = \frac{\nu}{\lambda/(\rho C_p)} = \frac{\mu C_p}{\lambda} = 1, \tag{5}$$

is used. The fluid is furthermore assumed to be calorically perfect and to obey the perfect gas law. The compressibility of the jet is parametrized by the Mach number. To keep the compressibility effects small a moderate Mach number is used. The inlet Mach number of the simulation is set to $M = U_J/a = 0.5$, where U_J is the inlet velocity at the jet center and a is the speed of sound at the inlet.

The mixing in the plane wall jet is studied by introducing a scalar in the simulation. The scalar is conserved i.e. no production or destruction of the scalar is present and the scalar is passive in the sense that the motion of the fluid is unaffected by the presence of the scalar. The equation governing the passive scalar concentration, θ, is of the form (see Poinsot and Veynante 2001),

$$\frac{\partial \rho\theta}{\partial t} + \frac{\partial}{\partial x_j}\left(\rho u_j \theta\right) = \frac{\partial}{\partial x_j}\left(\rho D \frac{\partial \theta}{\partial x_j}\right) \tag{6}$$

where D is the diffusion coefficient of the scalar. In the simulation the scalar diffusivity in terms of the Schmidt Sc number is

$$Sc = \frac{\nu}{D} = 1. \tag{7}$$

FLOW CONFIGURATION

The computational domain used in the simulation is a rectangular box. The physical domain size, in terms of the jet inlet height h, is $L_x/h \approx 37$, $L_y/h \approx 16$ and $L_z/h \approx 10$ in the streamwise, wall normal and spanwise directions respectively. The inlet of the jet is positioned directly at the wall with the flow directed along it. The Reynolds number of the jet is $Re_h = U_J h/\nu = 2000$ based on the inlet height h and jet inlet velocity U_J. Above the jet inlet a coflow of 10% of the jet inlet velocity is applied.

At the inlet, the streamwise velocity profile is assigned using a composite profile comprised of three parts. The inner part of the profile, extends from zero at the wall to the characteristic jet velocity at a point slightly below the center on the jet $y_{c1} = 0.46h$. The outer part of the profile extends from a point above the jet center $y_{c2} = 0.54$ out to the very top of the domain, containing both the top part of the jet and the coflow region above the jet. The inner and outer profiles are joined by a third profile covering only the center of the jet between the two connecting points y_{c1} and y_{c2}. For the inner and outer profiles hyperbolic tangent functions are used while the center profile is a second order polynomial. The functions are curve fitted to preserve the first derivative at the connecting points.

The inlet shape of the passive scalar is prescribed using a profile of the shape

$$\theta_{in} = \frac{\theta_J}{2}(1 - \tanh\left(G_i\left(\sqrt{y^2} - h_\theta\right)\right)) \tag{8}$$

where θ_J is the scalar concentration at the wall position, G_i determines the profile steepness and $h_\theta = 0.9h$ is the scalar inlet height. The resulting profile is finite at the wall and zero above the jet i.e. no coflow condition is used for the scalar.

NUMERICAL METHOD

The computational domain is discretized using a structured grid. The grid employed is stretched in the wall normal direction, clustering nodes close to the wall, but uniform in the streamwise and spanwise direction. The number of nodes used in the present simulation is $256 \times 192 \times 96$, in the streamwise, wall normal and spanwise direction respectively. In the simulation, the streamwise and the wall normal directions are non-periodic, while the spanwise direction is treated periodically. On the wall a no-slip condition is set for the velocities and a no-flux condition is used for the scalar.

For the spatial integration of the governing equations a compact finite difference scheme in the manner of Lele (1992) is employed. The scheme is tridiagonal and of eighth order of accuracy. In the non-periodic directions schemes of reduced order are used for the nodes close to the boundary. At the node directly at the boundary, a one-sided third order scheme is used. At the two consecutive nodes, schemes with reduced stencils are used before the inner full sized scheme can be utilized in the interior domain. The order of accuracy in the nodes with reduced stencil is fourth and sixth respectively.

For the temporal integration an explicit Runge-Kutta scheme of third order is employed. The scheme is on low-storage form and is presented in Lundbladh et al. (1999).

In the wall jet simulation, boundary zones in the manner of Freund (1997) are used to minimize the reflection and generation of spurious waves at the boundaries. Waves of this type are non-physical artifacts of numerical simulations and an effort should be made to prevent them from propagating back and interacting with the interior flow. Many different techniques have been proposed for this purpose, but in the case where large disturbances are to pass the boundary with minimal reflection, which is the case at the outflow of the wall jet, it has been found necessary to add boundary zones or absorbing layers adjacent to the boundaries. Following the method of Freund (1997), two additional terms, one convective and one dissipative, are added smoothly to the equations in the vicinity of the inlet and the outlet.

At the inlet, incoming disturbances are generated using a filter method developed by Klein et al. (2003). The method uses a prescribed autocorrelation and a characteristic length scale of the disturbances to generate a digital filter. The characteristic length scale of the disturbances is set to $h/3$. The inlet disturbances are applied at the jet inlet where $y \leqslant h$ with a root mean square value of 20% of the inlet jet velocity. The implementation of the digital filter is not yet optimal and will be improved.

WALL JET DEVELOPMENT

The downstream development and the turbulent structure of the simulated wall jet is presented in figures 1 to 4. To account for the slight compressibility, all the mean and fluctuating profiles of simulation have been produced using mass-averaging. Comparisons of the simulation are made with the experimental data of Eriksson et al. (1998). Their data are however acquired at an inlet Reynolds number of $Re = 9600$, which is a factor of 4.8 higher than that of the simulation. The experimental data are very well resolved, also close to the wall, which facilitates a comparison of the properties in the inner and outer shear layers of the jet by employing different scaling methods.

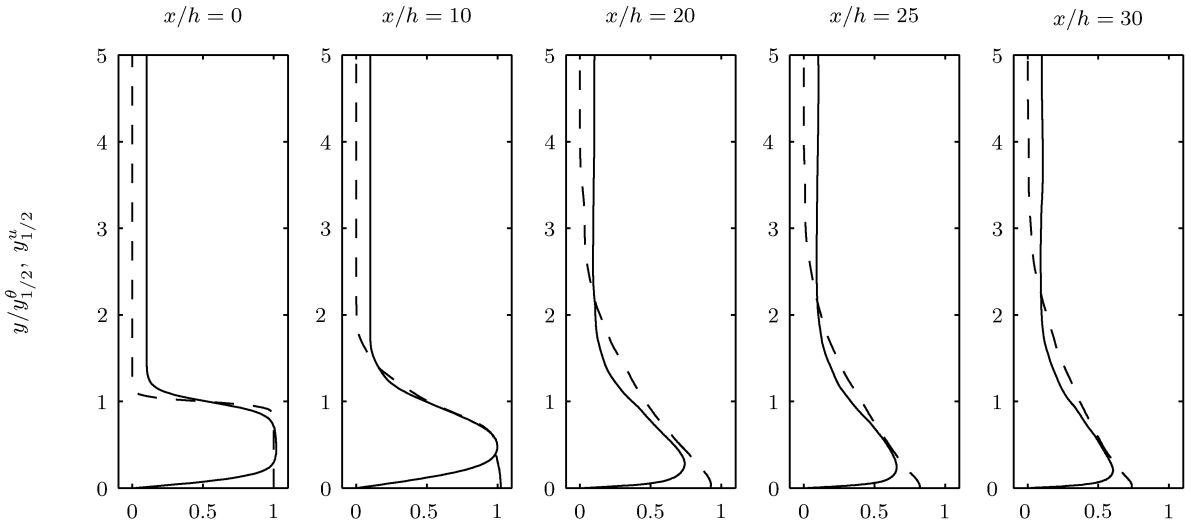

Figure 1: Inlet normalized mean streamwise velocity ($\tilde{U}/\tilde{U}_J$), (—) and scalar concentration ($\tilde{\theta}/\tilde{\theta}_J$), (- -) at different downstream positions

The downstream development of the jet is presented in figure 1, where the mean streamwise velocity and scalar concentration are plotted at various downstream positions. The profiles are normalized by the inlet conditions and plotted against the wall normal distance, scaled with an outer length scale. The outer length scale used for the velocity is the jet half-width, $y^u_{1/2}$, which denotes the distance from the wall to the position where the mean velocity has decreased to half of its maximum value. The jet half-width characterizes the position of the outer shear layer and is often used to describe the growth of the wall jet. In analogy, an outer length for the scalar in the form of the scalar half-width $y^{\theta}_{1/2}$ is used for the scalar concentration profiles, where the scalar half-width is defined as the distance from the wall to the position with half of the maximum concentration.

By observing the velocity profiles, it is concluded that a significant part of the domain is taken up by the transition to a fully turbulent state. At the position $x/h = 10$ the velocity profiles are still of laminar type, while at $x/h = 20$ and downstream the profiles appear turbulent.

From the scalar concentration profiles it is seen that the mixing occurs earlier in outer shear layer compared to close to the wall. This is a natural consequence of the inlet mean scalar profile, and the fact that large roll-up structures appear in the upper shear layer also prior to the turbulent propagation.

The growth rate of the jet is shown in figure 2 where the velocity and scalar jet half-widths normalized by the inlet height h are plotted for increasing donwstream positions and compared to the experimental results of Eriksson et al. (1998). Looking at the velocity, the simulated growth is seen to be slower in the first part of the domain, but develops an approximately linear growth relation downstream of $x/h = 15$. The conclusion of a linear growth must be taken with some caution due to the limited simulation length.

Downstream of the transition, the growth rate is found to be somewhat faster than the one present in the experiments. This effect is most probably related to the lower Reynolds number of the simulation, which from the smaller difference in scale sizes in the respective layers, enable the inner layer to influence the outer layer to a larger extent. The scalar half-

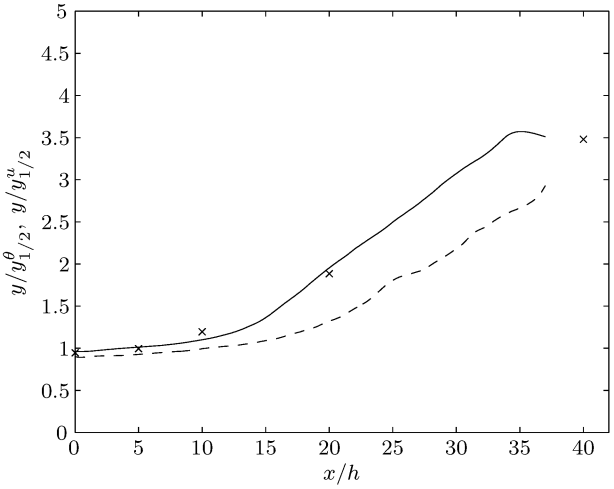

Figure 2: Wall jet growth rate in terms of the velocity (–) and scalar half-width (- -) of the DNS compared to the experimental velocity half-width (×) of Eriksson et al. (1998)

width from the simulation is positioned below the velocity and requires an extended distance, approximately $x/h = 20$, before an approximately linear growth is reflected in the development.

Profiles of the rms of the velocity fluctuations and the scalar concentration fluctuation, using different scaling methods, are presented in figures 3-4. In figure 3 the wall normal fluctuation is compared to the experiments at two downstream positions of $x/h = 20$ and $x/h = 40$. Since the computational domain is not large enough to contain the second point the simulation data are taken at $x/h = 30$, which is considered to be the last position not affected by the outlet boundary zone. In the upper two figures inner scaling is used for the wall normal fluctuations $v^+ = v''/u_\tau$ and the wall normal distance $y^+ = yu_\tau/\nu$, where u_τ is the friction velocity. The inner scaling is seen to approximately collapse the simulation and experimental data in the inner layer. A full collapse is prevented by the fact that the experimental data

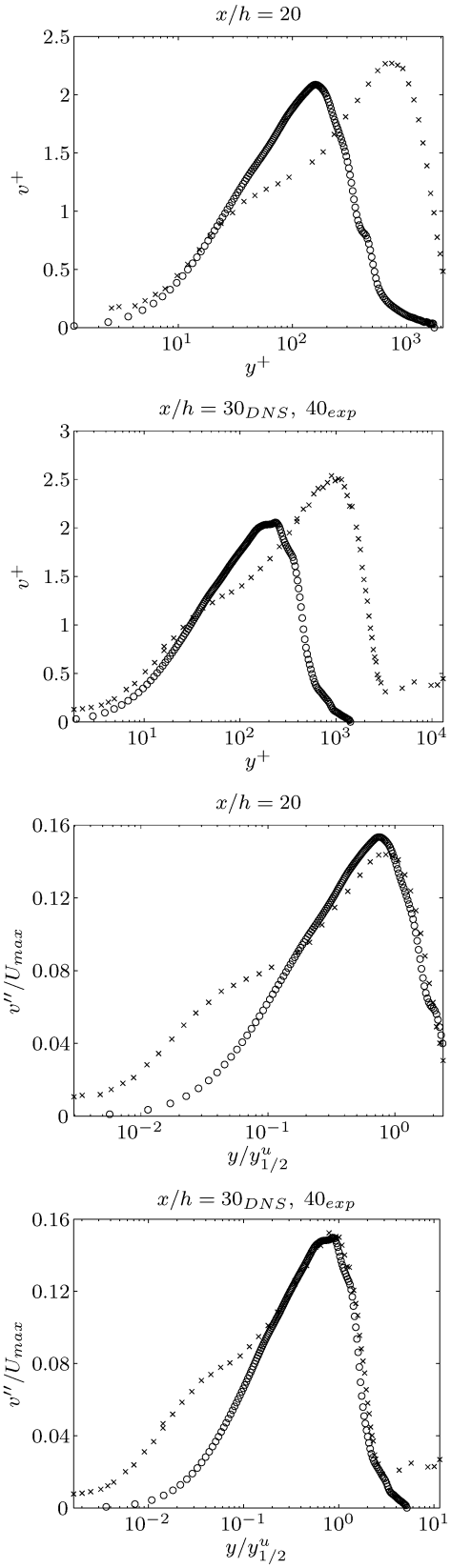

Figure 3: Comparison of wall normal velocity fluctuations from DNS, (o), and experiments, ($\times$), by Eriksson et al., using inner (upper two) and outer scaling (lower two)

does not approach zero at the wall. Only the inner part can be collapsed using this scaling since the Reynolds numbers are significantly different. The higher Reynolds number of the experiments yields a broader profile extending into higher y^+ values as well as a plateau joining the inner and outer parts of the jet. The reason for the plateau can be argued to be a scale separation, where the large fluctuations of the outer layer are positioned further out and contrasted to the smaller scales of the inner boundary layer type shear layer. The absence of the plateau in the DNS is thus explained by the lower Reynolds number. In the lower two figures, an outer scaling is employed by scaling the velocity by the maximum velocity U_m and the wall distance by the jet half width. The outer scaling is found to approximately collapse the outer part of the jet. At the most downstream position the profiles seem to collapse very well, but it must be kept in mind that the experimental data are taken at a further downstream position.

Further information on the turbulent correlations are given in figure 4 where the streamwise velocity fluctuation u'' and the shear stress $\overline{\rho u'' v''}$ are plotted using inner scaling. The streamwise fluctuations can be seen to have a two-peak structure corresponding to the inner and outer layers, where the inner and outer peaks are both approximately of the same order. The shear stress has a negative inner part and a positive outer. The point of vanishing shear stress is found to be approximately at $y^+ = 40$, which is positioned below the point of maximum streamwise velocity. For the profile at $x/h = 25$ the shear stress vanishes at $y^+ = 45.1$ while the maximum velocity is positioned at $y^+ = 58.0$. This displacement is a well known feature of the wall jet and is discussed in Launder and Rodi (1983).

WALL JET MIXING

The fluctuation of the scalar concentration is shown in figure 5, where the unscaled fluctuation is plotted against the wall distance in outer scaling. It can be seen that the scalar fluctuation originally grows separately in the inner an outer shear layer. Further downstream, in the fully developed wall jet, the fluctuations are merged into a single peak shape. The low level of scalar fluctuations in the inner layer for low x/h is explained by the fact that the mean scalar is almost constant close to the wall. For low x/h the outer peak is positioned at the scalar half-width $y^\theta_{1/2}$ while after the merging, through the influence of the inner layer, the combined peak is positioned closer to the wall in terms of the half-width.

The turbulent scalar flux, $\overline{\rho u_i'' \theta''}$, provides a direct measure on how the scalar concentration is redistributed by the turbulent velocity fluctuations. Profiles for the wall normal scalar flux, normalized by the mean density and the local maxima of the streamwise velocity and the scalar concentration, are plotted in figure 6. It is seen that scaling the wall distance with the scalar half-width produces an approximate collapse in the outer layer. In the inner layer however, the profiles do not collapse, which on the other hand would not be expected from an outer scaling. Instead the flux is found to increase downstream as the mean scalar gradient close to the wall increases. The outer flux peaks at the far downstream positions are situated close to the scalar half-width, only slightly displaced in the direction towards the wall, approximately at $y/y^\theta_{1/2} = 0.9$, from this property and the substantial difference in magnitude, the mixing in the wall jet is concluded to be dominant in the outer layer with only a small influence from the inner one. This fact

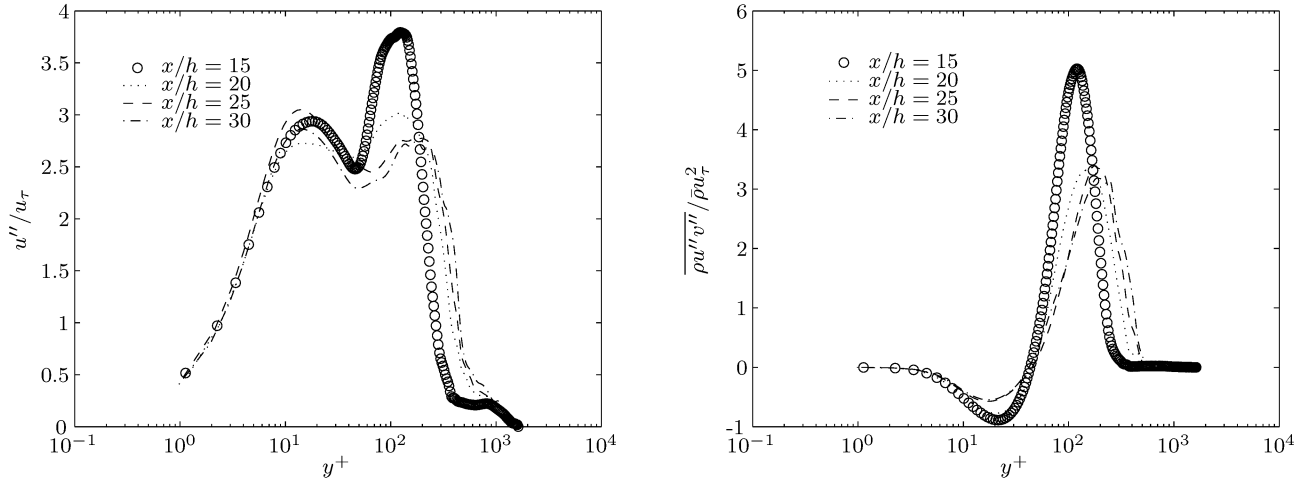

Figure 4: Streamwise velocity fluctuations (left) and shear stress (right)

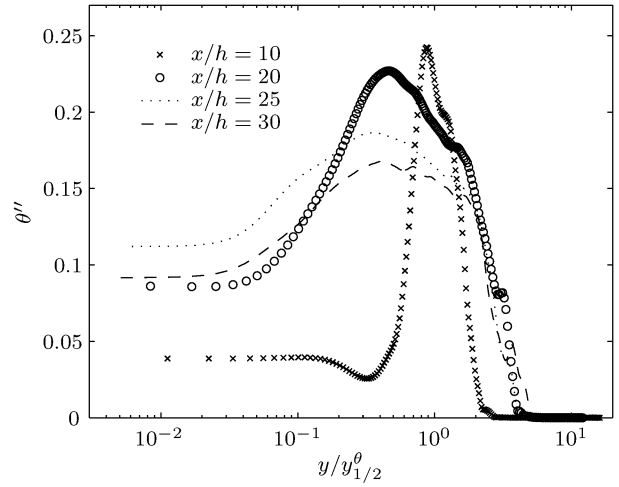

Figure 5: Scalar fluctuation

is of course enhanced by the absence of mean scalar variation close to the wall.

The mixing in the inner and outer shear layers is further characterized by probability density functions. In figure 7 the pdf of the scalar concentration, scaled by the local mean concentration, is plotted at two wall normal distances, one in the inner shear layer at the position of the inner peak of streamwise velocity fluctuation u'', and a second one in the outer layer at the position of the scalar half-width $y/y^\theta_{1/2} = 1$.

The pdfs in the inner and outer layers have a distinctly different shape. The inner pdf is narrower, particularly so at the first two downstream positions. This clearly indicates that the mixing is less intense at the inner position compared to the outer. Moving further downstream, the width of the pdf, and hence the mixing at the inner position can be seen to increase. These two properties were also seen looking at the scalar fluctuation in figure 5. The shape of the pdf in the outer part does not change in the same manner as the inner one, indicating a more constant mixing situation. The shape of the outer profile is also more Gaussian like and the mixing at this position is hence interpreted as more homogeneous than at the inner position.

The joint pdf of the wall normal velocity fluctuation and the scalar concentration is shown in figure 8, where scaling by the local velocity rms and mean concentration have been used. The left figure shows the contours of the joint pdf at the same inner position used in the previous single pdfs and the right one at the corresponding outer position. Both pfds are acquired in the far end of the domain at $x/h = 30$. At the inner position the velocity and the concentration are seen to be uncorrelated since the pdf is aligned in the vertical direction. The outer pdf exhibits a positive inclination which imply a positive correlation i.e. that low concentration fluid is correlated to a velocity fluctuation towards the wall and vice versa.

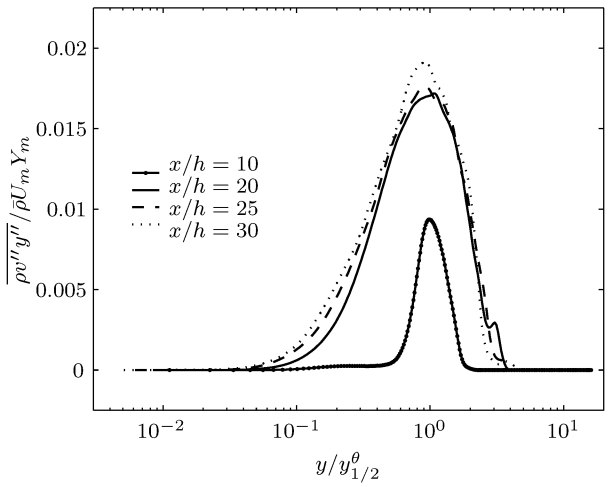

Figure 6: Turbulent scalar flux

CONCLUDING REMARKS

The present paper describes the efforts in a first step towards direct numerical simulation of reactive flows with special emphasis on wall effects. Main results of the presented simulation include the observed scaling of the inner and outer parts of the plane wall jet by a corresponding inner and outer scaling. This confirms the inner and outer shear layer structure of the wall jet. A corresponding inner and outer layer dependence is also found for the passive scalar mixing, where mixing in the outer part is dominant.

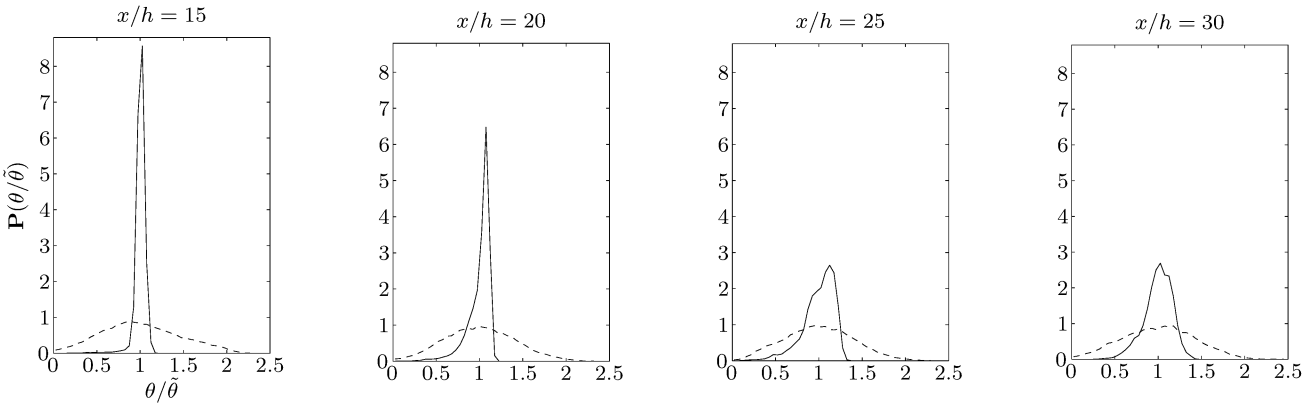

Figure 7: Pdfs of the scalar concentration, scaled by the local mean, at wall normal distances corresponding to (—) $u'' = u''_{inner\ peak}$ and (- -) $y/y^{\theta}_{1/2} = 1$

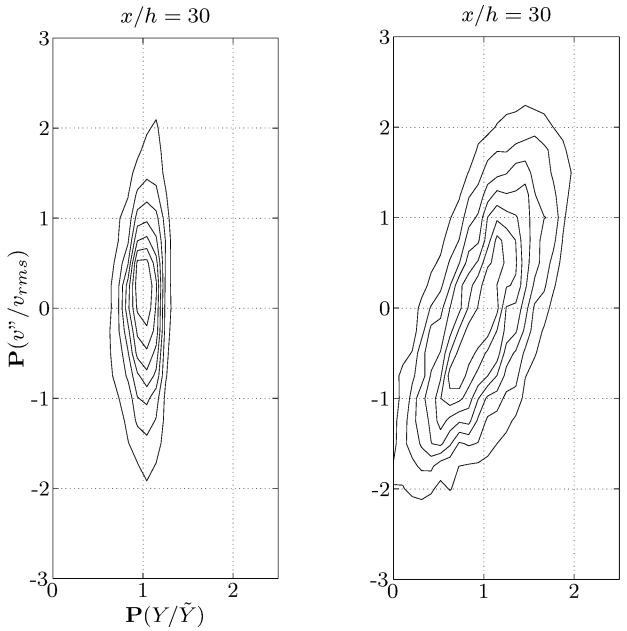

Figure 8: Joint pdfs of the wall normal fluctuations, scaled by the local rms-value, and the scalar concentration, scaled by the local mean, acquired at wall normal distances corresponding to $u'' = u''_{inner\ peak}$ (left) and $y/y^{\theta}_{1/2} = 1$ (right)

REFERENCES

Eriksson, J.G., Karlsson, R.I. and Persson J., 1998, "An experimental study of a two-dimensional plane turbulent wall jet", *Experiments in Fluids*, Vol. 25, pp. 50-60.

Freund, J.B., 1997, "Proposed Inflow/Outflow Boundary Condition for Direct Computation of Aerodynamic Sound", *AIAA Journal*, Vol. 35, pp. 740-742.

George, W.K., Abrahamsson, H., Eriksson, J., Karlsson, R.I., Löfdahl, L., and Wosnik, M., 2000,"A similarity theory for the turbulent plane wall jet without external stream", *Journal of Fluid Mechanics*, Vol. 425, pp. 367-411.

Klein, M., Sadiki, A. and Janicka, J., 2003, "A digital filter based generation of inflow data for spatially developing direct numerical or large eddy simulations", *Journal of Computational Physics*, Vol. 186, pp. 652-665.

Launder, B.E. and Rodi, W., 1981, "The turbulent wall jet", *Progress in Aerospace Sciences*, Vol. 19, pp. 81-128.

Launder, B.E. and Rodi, W., 1983, "The turbulent wall jet - measurements and modeling", *Annual Review of Fluid Mechanics*, Vol. 15, pp. 429-459.

Lele, S.K., 1992, "Compact finite differences with spectral-like resolution", *Journal of Computational Physics*, Vol. 103, pp. 16-42.

Lundbladh, A., Berlin, S., Skote, M., Hildings, C., Choi, J., Kim, J. and Henningson, D., 1999, "An Efficient Spectral Method for Simulation of Incompressible Flow over a Flat Plate", Technical Report 1999.11, TRITA-MEK, Royal Institute of Technology, Stockholm

Poinsot, T and Veynante, D., 2001, *Theoretical and Numerical Combustion*, R.T. Edwards, Philadelphia, PA

Stanley, S.A., Sarkar, S. and Mellado , J.P., 2002, "A study of the flow field evolution and mixing in a plane jet using direct numerical simulation", *Journal of Fluid Mechanics*, Vol. 450, pp. 377-407.

Wygnanski, I., Katz, Y., and Horev, E., 1992, "On the applicability of various scaling laws to the turbulent wall jet", *Journal of Fluid Mechanics*, Vol. 234, pp. 669-690.